CHAPTER IV

DISCUSSION

4.1 MECHANICAL PROPERTIES

The uniaxial tensile behaviors of specimens are remarkably different (Table 4-1). The specimen A has a higher yield strength and tensile strength than both that of the specimen B and C, and the ductility of the specimen A is lower than that of the other two kinds of specimen. This result can be explained by the strain-hardening theory for the steel sheet - the strain-hardened material has a higher yield point and a higher tensile strength, but lower ductility.

Table 4-1 Mechanical properties of samples

Specimen	Yield strength (MPa)	Tensile strength (MPa)	Elongation %
A	484.8	613.2	5.0
B	368.6	393.8	13.6
C	266.7	381.5	27.3

The stress-strain curve (Fig.4-1) of the specimen C contains a lower yield strength and lower tensile strength, and a high value of elongation. The

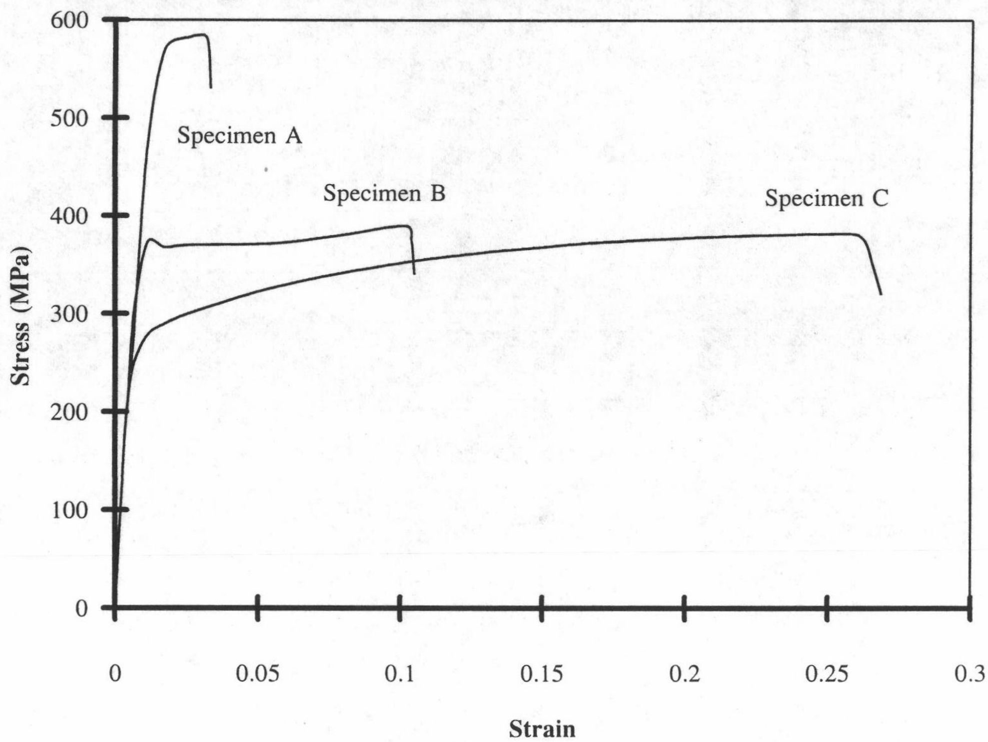

Fig.4-1 Comparison of the stress-strain curve of three kinds of specimens

stress-strain curve shows that an evidently yield strain exists in the specimen B, but not in the specimen C. Usually the yield point can be associated with small amounts of interstitial or substitutional impurities. The almost complete removal of carbon and nitrogen from low-carbon steel sheets by wet-hydrogen treatment will remove the yield point. However, only about 0.001 percent of either of these elements is required for a reappearance of the yield point. The explanation of this behavior is one of the early triumphs of dislocation theory. Carbon or nitrogen atoms in iron readily diffuse to the position of minimum energy just below the extra plane of atoms in a positive edge dislocation. The elastic interaction is so strong that the impurity atmosphere becomes completely saturated and condenses into a row of atoms along the core of the dislocation. When the dislocation line is pulled free from the influence of the solute atoms, slip can occur at a lower stress. Alternatively, where dislocations are strongly pinned, such as by carbon and nitrogen in iron, new dislocations must be generated to allow the flow stress to drop. This explains the origin of the upper yield stress (the drop in load after yielding has begun). The dislocations released into the slip plane pile-up at the grain boundaries. The pile-up produces a stress concentration at its tip which combines with the applied stress in the next grain to unlock sources (or create new dislocations). (George E.Dieter,1986)

Stability ratio (SR), a measure of the degree to which the interstitial atoms are free, was calculated by the following relationship: SR = {(Nb) /92.9 + [(Ti) - 48/32(S) - 48/14(N)]/47.9}/[(C) /12.01], where ( ) is weight percent of the alloying element. A calculated value of SR>1 implies there are no free interstitial atoms, and the steel is thus referred to as stabilized; SR<1 refers to an unstabilized steel. Table 4-2 gives the stability ratio of specimen B and specimen C. The values of stability ratio of

Table 4-2 Stability ratio of specimens

Sample	Nb%	Ti%	S%	N%	C%	SR
B	.00104	.001	.0027	.00601	.0442	-0.131
C	.00102	.001	.0066	.00459	.0792	-0.076

the samples show that both kinds of specimens are unstabilized steels and the specimen B has the more free interstitial atoms than that of the specimen C. It means that in specimen B strain aging occurs more easily than that of the specimen C.

During the rolling process, the steel sheets are strained plastically through the yield-point elongation to the desired strain. The dislocations have been torn away from the atmosphere of carbon and nitrogen atoms. Annealing process, in which steel sheets are heated to the annealing temperatures, causes the carbon and nitrogen atoms to diffuse to the dislocations during the aging period to form new atmospheres of interstitial anchoring the dislocations.

For the specimen B and C, the temper rolling method was used after annealing. One of the effects of temper rolling is to remove the sharp yield point present in most commercial annealed steels. Less strain is required to eliminate the yield point by temper rolling than by stretching the steel under tension. The temper rolling gives rise to very narrow alternating bands of deformed and undeformed metal running transverse to the rolling direction(shown in Fig.4-2). On a larger scale, these bands produce a relative uniformity of yielding in the steel or strip. Under conditions of stretching, however, the strain to produce uniform yielding must exceed the yield elongation.

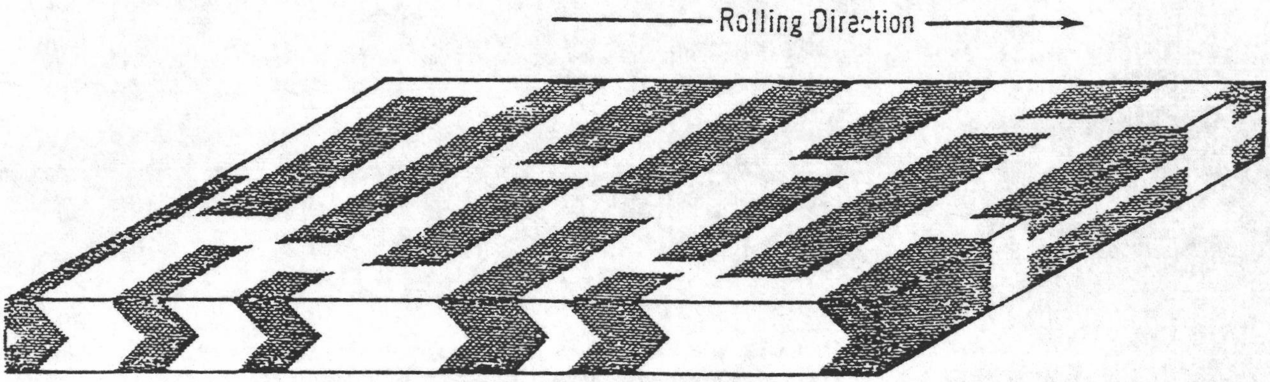

Fig.4-2 Schematic diagram showing the distribution of deformed and undeformed regions formed during a light temper rolling
(From "Temper Rolling and Its Effect on Stretcher-Strain Sensitivity" E.J.Paliwoda, 1960)

Although the steel sheets are temper rolled after annealing for removing the yield point, steel sheets are maintained at room temperature for prolonged periods, the sharp yield point may be appear. This behavior can best be explained by strain aging of the steel sheets. Strain aging is a type of behavior, usually associated with the yield point phenomenon, in which the strength of a metal is increased and the ductility is decreased. Moreover, other properties that affect drawability are impaired. Table 4-3 shows the change of hardness for each kind of specimen, it also shows the degree of strain aging.

Table 4-3 Hardness of the specimens

Specimen	Hardness HR 30-T	
	After temper rolling	Present-day
A	73	75.8
B	61	67.1
C	57	57.7

For studying strain aging characteristics of the specimen B and C, the value of aging index (AI) was evaluated by measuring the stress difference between the flow stress at 5% prestrain and the lower yield stress after aging 100°C for 60 minutes (shown in Fig.4-3). In this test, the standard sheet-type

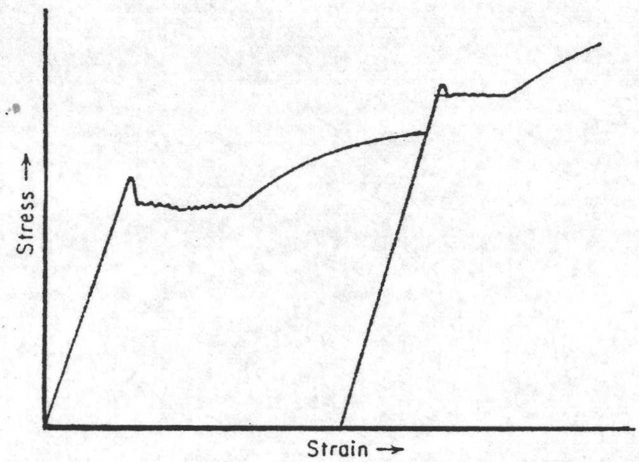

Fig.4-3 Stress-strain curve for calculating AI

specimens (ANSI/ASTM A 370-77) were pulled to 5% strain and the flow stress was recorded. Then the specimens were unloaded and heated at 100°C for 60 minutes (aging treatment). The aged specimens were pulled again, and the lower yield stresses and yield elongations were recorded. The conclusion of strain aging characteristics (Table 4-4) shows that the specimen C has a better anti-strain aging property with a lower AI (6.49 MPa) and a lower yield elongation (<0.2%) than that of the specimen B with a AI (18.96 MPa) and a yield elongation (1.2%).

Table 4-4 Strain aging characteristics

Specimen	Aging index (MPa)	Yield elongation %
B	18.96	1.2
C	6.49	<0.2

Strain aging is attributable to the segregation of interstitial atoms at the dislocation formed during temper rolling. These so-called atmospheres pin the dislocation restraining their movement and hence recreating the sharp yield point. The amount of interstitial atoms dissolved in the ferrite and the type of prestrain are the most important factors affecting strain aging. The rate of strain aging increases if the amount of interstitial atoms or reduction of prestrain increase.

4.2 PLANE-STRAIN TENSILE TEST AND FORMING LIMIT DIAGRAM

The forming limit diagrams (left hand) of three kinds of specimens (Fig.4-4) have the similar shape. The difference of the FLD's can be shown by the intercept of the FLD's on the major strain axis and the end point of the FLD's.

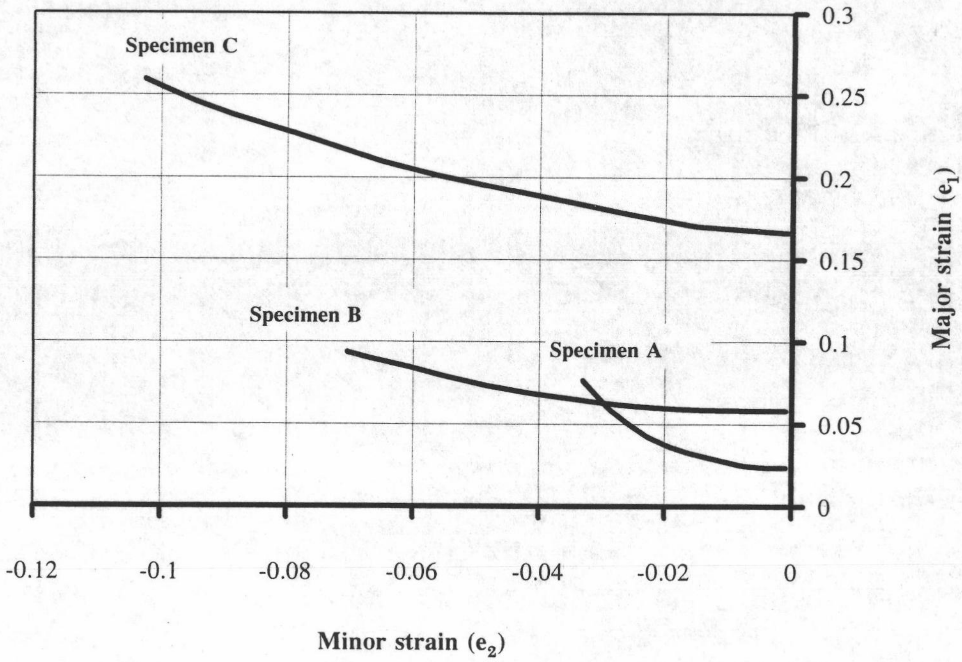

Fig.4-4 Comparison of the forming limit diagram of three kinds of specimens

The intercept of the FLD's on the major strain axis shows the limit strain under plane-strain tensile condition and the end point of the FLD's shows the limit strain under the condition similar to the uniaxial tension.

Work by Keeler and Brazier (1977) and Buncher (1977) showed that the intercept of the FLD on the major strain axis is a function of the sheet thickness and the strain-hardening exponent. The intercept of the FLD on the major strain axis moves up if the value of thickness and strain-hardening exponent increase. They also showed that the FLD is affected only slightly by variables such as composition, specimen

Table 4-5 Mechanical properties of samples

Specimen	Thickness (mm)	n Uniaxial tension	n Plane-strain	Elongation %
A	0.18	0.0513	0.057	5.0
B	0.20	0.1035	0.1103	13.6
C	0.22	0.24	0.255	27.3

orientation relative to the sheet rolling direction, inclusion distribution and plastic strain ratio, which were previously believed to control forming characteristics. Because these variables strongly influence the value of n, their effect on forming characteristics is indirect.

Table 4-5 shows the thickness, strain-hardening exponent, and limit strain of the specimens under the uniaxial tensile tests.

During the plane-strain tensile tests, it is noticed that the crack occurs at the center of the specimen, which is under a pure plane-strain state (shown in Fig.4-5). It shows that plane-strain state, without strain in width direction of the specimen, is one of the most critical strain state. It can be explained by the theory of volume constant - $e_1+e_2+e_3=0$, where e_1 is strain in the tensile direction, e_2 is strain in the width direction, and e_3 is strain in the thickness direction. The value of major strain, $e_1=-(e_2+e_3)$, will be the minimum value if $e_2=0$.

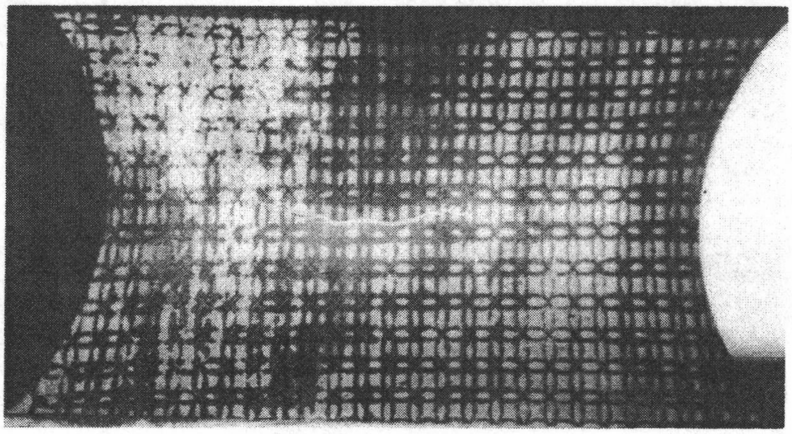

Fig.4-5 Cracks occurred in the mid area of specimen which was in plane-strain state

4.3 DRAWING TEST

The limit drawing ratio increases with increasing normal anisotropy, R, and thickness. The high R-value should investigate that the material has a high thinning resistance. That means the ratio of the true strain in the width direction to the true strain in the thickness direction of plastically strained steel sheet is high. The R-values and limit drawing ratio of three kinds of specimens are listed in Table 4-6.

Table 4-6 Limit drawing ratio

Specimen	Thickness, mm	Anisotropy, R	LDR
A	0.18	1.44	1.44
B	0.20	1.69	1.80
C	0.22	1.88	2.19

The typical mechanical properties of the three kinds of low-carbon steel sheets are shown in Fig.4-6. The relationships between the limit drawing ratio and the typical mechanical properties shows that the limit drawing ratios vary with the mechanical properties. The limit drawing ratios increase with the decrease of yield strength and hardness, and the increase of elongation.

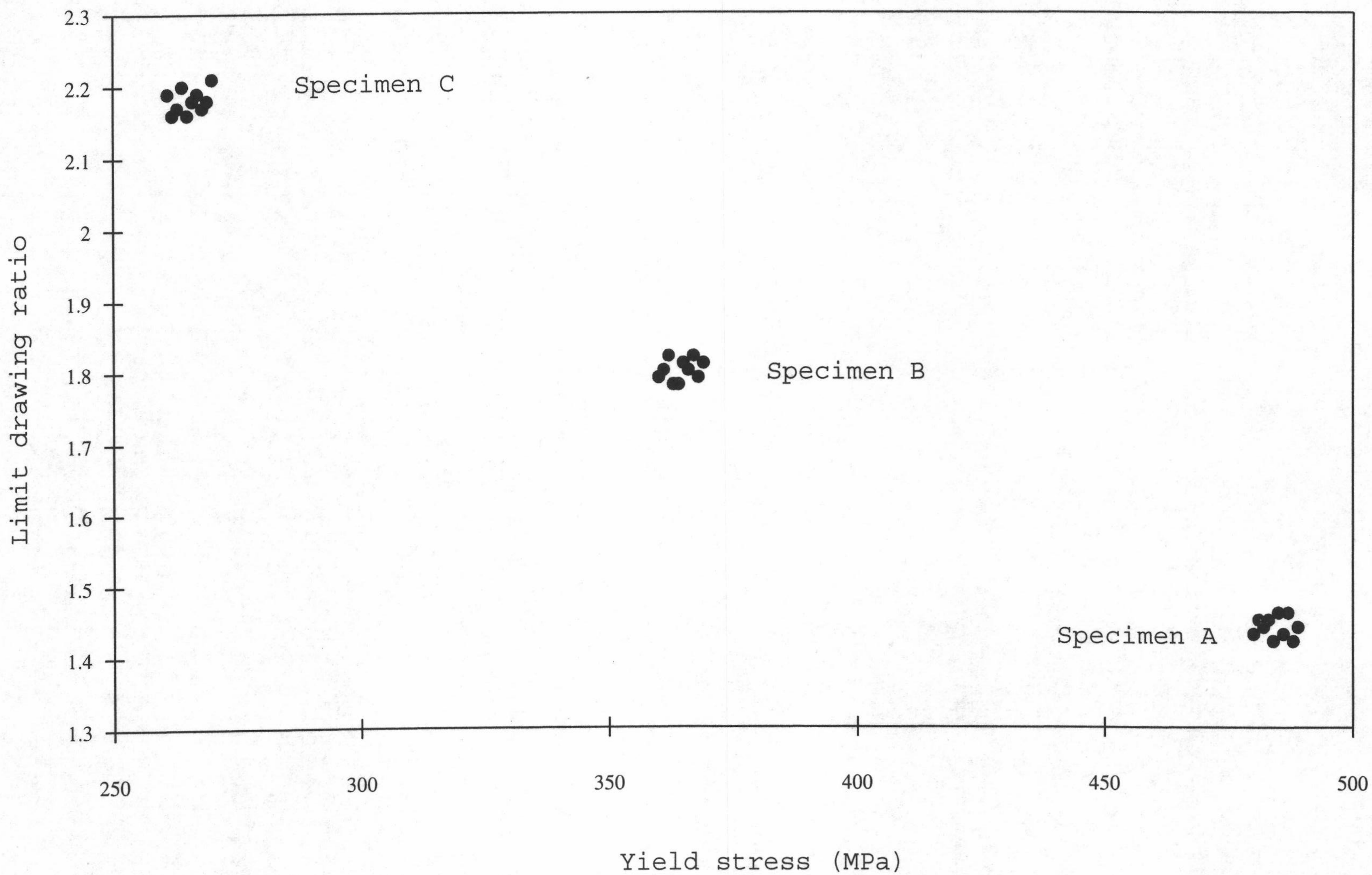

Fig.4-6 Relationship of LDR and mechanical properties

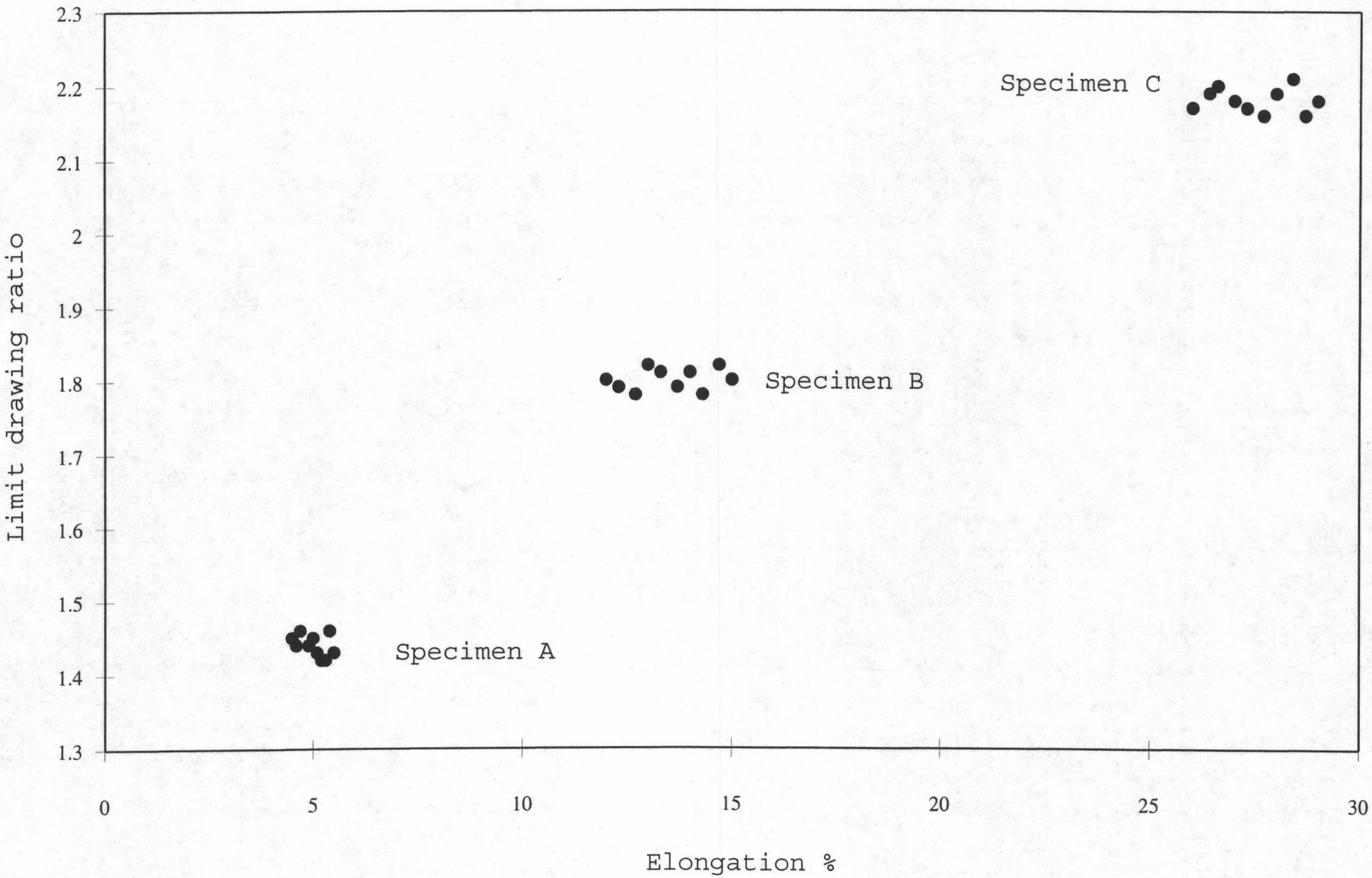

Fig.4-6 Relationship of LDR and mechanical properties (continue)

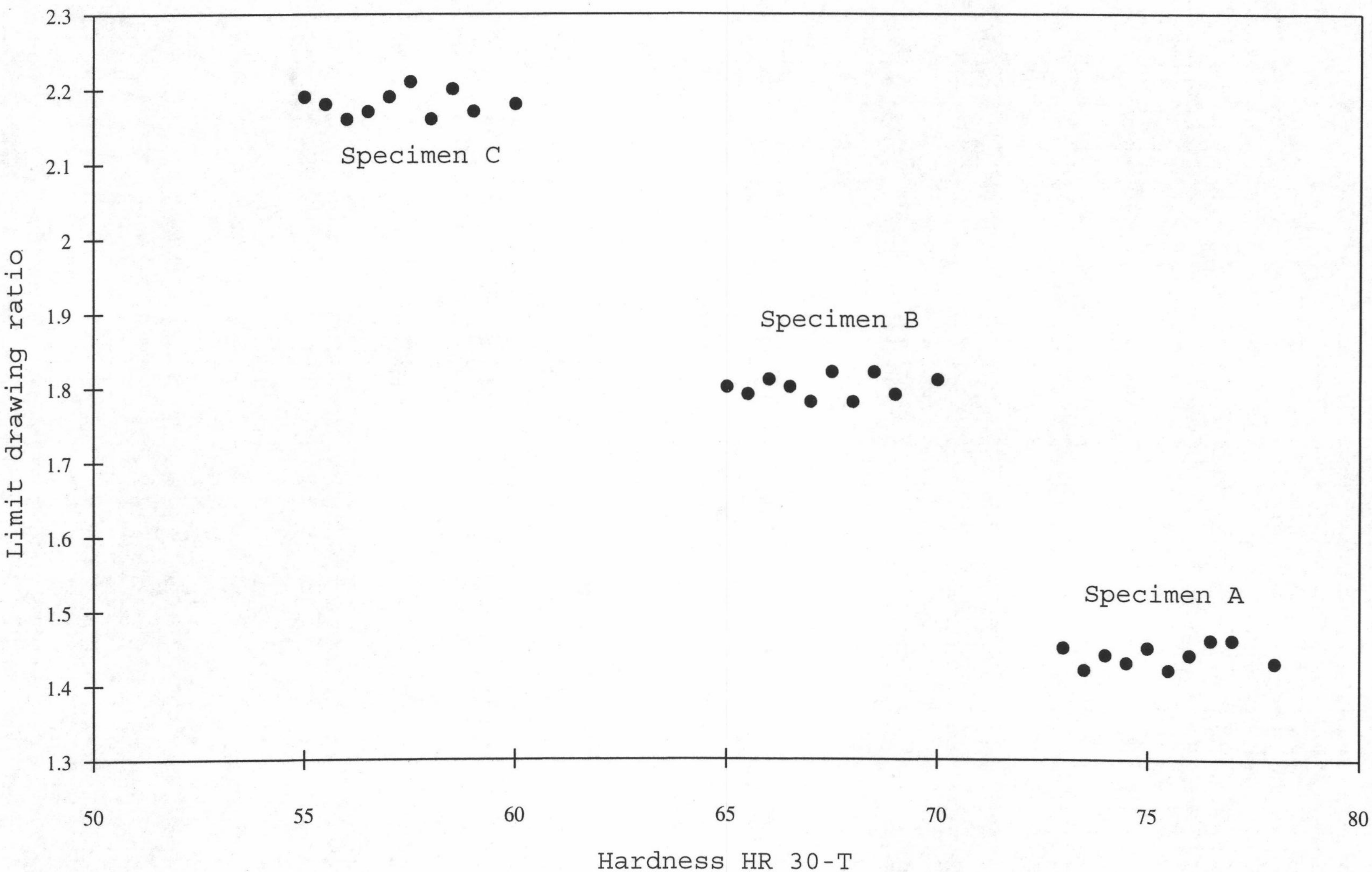

Fig.4-6 Relationship of LDR and mechanical properties (continue)